THE JOURNAL OF BIOLOGICAL CHEMISTRY VOL. 290, NO. 41, pp. 24793–24805, October 9, 2015

Transcription Factor Hepatocyte Nuclear Factor-1β (HNF-1β) Regulates MicroRNA-200 Expression through a Long Noncoding RNA*

Received for publication, June 6, 2015, and in revised form, August 18, 2015 Published, JBC Papers in Press, August 19, 2015, DOI 10.1074/jbc.M115.670646

Sachin S. Hajarnis[‡], Vishal Patel[‡], Karam Aboudehen[‡], Massimo Attanasio[‡], Patricia Cobo-Stark[‡], Marco Pontoglio[§1], and Peter Igarashi[‡¶2]

From the Departments of [‡]Internal Medicine and [¶]Pediatrics, University of Texas Southwestern Medical Center at Dallas, Dallas, Texas 75390 and [§]Département de Génétique et Développement, INSERM U1016, CNRS UMR 8104, Université Paris-Descartes. Institut Cochin, 75014 Paris, France

Background: Transcription factor HNF-1β regulates epithelia-specific gene expression.
Results: Mutations of HNF-1β down-regulate the miR-200b/200a/429 miRNA cluster and increase expression of *Zeb2* and *Pkd1*.
Conclusion: HNF-1β directly activates the transcription of a lncRNA encoding miR-200b/200a/429.
Significance: A novel mechanism whereby mutations of HNF-1β produce kidney cysts and epithelial-mesenchymal transition was identified.

The transcription factor hepatocyte nuclear factor-1β (HNF-1β) regulates tissue-specific gene expression in the kidney and other epithelial organs. Mutations of HNF-1β produce kidney cysts, and previous studies have shown that HNF-1β regulates the transcription of cystic disease genes, including *Pkd2* and *Pkhd1*. Here, we combined chromatin immunoprecipitation and next-generation sequencing (ChIP-Seq) with microarray analysis to identify microRNAs (miRNAs) that are directly regulated by HNF-1β in renal epithelial cells. These studies identified members of the epithelial-specific miR-200 family (miR-200b/200a/429) as novel transcriptional targets of HNF-1β. HNF-1β binds to two evolutionarily conserved sites located 28 kb upstream to miR-200b. Luciferase reporter assays showed that the HNF-1β binding sites were located within a promoter that was active in renal epithelial cells. Mutations of the HNF-1β binding sites abolished promoter activity. RT-PCR analysis revealed that a long noncoding RNA (lncRNA) is transcribed from the promoter and encodes the miR-200 cluster. Inhibition of the lncRNA with siRNAs decreased the levels of miR-200 but did not affect expression of the *Ttll10* host gene. The expression of the lncRNA and miR-200 was decreased in kidneys from HNF-1β knock-out mice and renal epithelial cells expressing dominant-negative mutant HNF-1β. The expression of miR-200 targets, *Zeb2* and *Pkd1*, was increased in HNF-1β knock-out kidneys and in cells expressing mutant HNF-1β. Overexpression of miR-200 decreased the expression of *Zeb2* and *Pkd1* in HNF-1β mutant cells. These studies reveal a novel pathway whereby HNF-1β directly contributes to the control of miRNAs that are involved in epithelial-mesenchymal transition and cystic kidney disease.

Hepatocyte nuclear factor-1β (HNF-1β,[3] vHNF1) is a transcription factor that belongs to the HNF-1 family of proteins. HNF-1β is expressed in epithelial organs, including liver, kidney, pancreas, gut, lung, and genital tract (1, 2). HNF-1β consists of 557 amino acids comprising an N-terminal dimerization domain, a DNA binding domain, and a C-terminal transactivation domain (3, 4). HNF-1β is required for tissue-specific gene expression and recognizes the consensus sequence 5′-GTTAATNATTAAC-3′ in the promoters of target genes. HNF-1β binds to DNA as a homodimer or heterodimer with HNF-1α and can activate or repress gene transcription (5). In the kidney, HNF-1β is expressed in tubular epithelial cells in all nephron segments (2, 6). Studies performed in zebrafish (7), *Xenopus* (8), and mouse (9) demonstrated that HNF-1β is required for kidney development and nephron patterning (10). HNF-1β regulates the expression of kidney-specific genes such as the sodium-potassium-chloride cotransporter (*Nkcc2*), kidney-specific cadherin 16 (*Cdh16*), collectrin (*Tmem27*), and uromodulin (*Umod*) (5, 11–13). HNF1–1β also regulates the expression of renal organic anion transporters such as *Oat1*/*Slc22a6*, *Oat3*/*Slc22a8*3, and *Oat4/Slc22a11*, the renal urate transporter *Urat1*/*Slc22a12*, and renal sodium phosphate transporter 4 (*Npt4*/*Slc17a3*) (14–18).

In humans, mutation of *HNF1β* produces cystic kidney disease and early-onset diabetes mellitus, a syndrome called renal cysts and diabetes (RCAD) (19). Mutations or deletions of *HNF1β* have also been linked to renal hypoplasia, multicystic

* This work was supported, in whole or in part, by National Institutes of Health (NIH) Grants R37DK042921 (to P. I.), P30DK079328 (to P. I.), K08DK084311 (to V. P.), NIH Training Grant T32DK007257 (to P. I.). The authors declare that they have no conflicts of interest with the contents of this article.
[1] Supported by Fondation pour la Recherche Médicale (equipe FRM) and the Fondation Bettencourt-Schueller (Prix Coup d'Elan); European Community's Seventh Framework Programme FP7/2009 (agreement 241955, SYSCILIA).
[2] To whom correspondence should be addressed: Dept. of Medicine, University of Minnesota School of Medicine, 420 Delaware St. SE, MMC 194, Minneapolis, MN 55455. Tel.: 612-625-3654; Email: igarashi@umn.edu.

[3] The abbreviations used are: HNF-1, hepatocyte nuclear factor-1β; EMT, epithelial-mesenchymal transition; miRNA, microRNA; pri-miRNA, primary miRNA; Q-PCR, quantitative real-time PCR; lncRNA, long noncoding RNA; ChIP-Seq, chromatin immunoprecipitation and high-throughput sequencing.

renal dysplasia, and glomerulocystic kidney disease. Inactivation of HNF-1β or expression of dominant-negative mutant HNF-1β in the mouse kidney produces renal cysts. HNF-1β controls the transcription of cystic disease genes, including *PKHD1*, the gene mutated in autosomal recessive polycystic kidney disease (ARPKD), and *PKD2*, which is mutated in autosomal dominant polycystic kidney disease (13, 20, 21). Decreased expression of *PKHD1*, *PKD2*, and other cystic disease genes may contribute to renal cyst formation in individuals carrying *HNF1β* mutations. In addition, down-regulation of HNF-1β has been implicated in epithelial-mesenchymal transition (EMT) and renal fibrosis (22).

MicroRNAs (miRNAs) are short, noncoding RNAs that regulate post-transcriptional gene expression. MicroRNAs are encoded by genomic sequences located in the introns of protein-coding host genes (intragenic) or present as independent transcriptional units (intergenic). The biosynthesis of miRNAs initially involves transcription of a primary miRNA (pri-miRNA), which can be several kilobases in length (23). The pri-miRNA is processed in the nucleus by Drosha to form a pre-miRNA, which then enters the cytoplasm where it is processed by Dicer to produce the mature 20–22-nucleotide miRNA. The mature miRNA associates with members of the Argonaute family to form the miRNA-induced silencing complex, which binds to complementary sequences located primarily within the 3′-UTR of target mRNAs. Binding of the miRNA-induced silencing complex to a target mRNA leads to degradation of the transcript, inhibition of translation, and/or sequestration in P bodies (24, 25). Because individual miRNAs can target multiple different transcripts in the same pathway, miRNAs can provide coordinated regulation of biological processes.

Aberrant up-regulation or down-regulation of specific miRNAs has been observed in polycystic kidney diseases (26, 27). Inactivation of Dicer in the kidney leads to cyst formation, suggesting that miRNAs are essential for normal tubular homeostasis (28). Increased expression of miR-17∼92 is observed in multiple genetic models of PKD. Moreover, overexpression of miR-17∼92 in renal tubules is sufficient to produce kidney cysts, whereas kidney-specific inactivation of miR-17∼92 inhibits cyst growth (26). These findings suggest that miRNAs may play a pathogenic role in PKD. However, the mechanisms that regulate the expression of miRNAs in the kidney are poorly understood. Here, we used genome-wide sequencing to identify miRNAs that are regulated by HNF-1β in kidney cells. We found that HNF-1β directly regulates the expression of the kidney-enriched miR-200 family through a novel long noncoding RNA.

Experimental Procedures

Reagents and antibodies—Anti-HNF-1β (sc-22840 X), anti-Zeb2 (sc-48789), and normal rabbit IgG (sc-2027) were purchased from Santa Cruz Biotechnology. G418 sulfate was purchased from Thermo Fisher Scientific. DMEM low glucose medium (catalog #11885-084), mifepristone (catalog #H110-01), DNase I (catalog #18068-015), and Lipofectamine® 2000 (catalog #11668-019) were purchased from Life Technologies. miRNeasy Mini kits were purchased from Qiagen.

Cells and Animals—Mouse renal epithelial cells (53A cells) that express dominant-negative mutant HNF-1β (DN-HNF-1β) have been previously described (29). mIMCD3 cells, 53A cells, and HeLa cells were grown in DMEM low glucose medium supplemented with 10% FBS and maintained in 5% CO_2 atmosphere at 37 °C. Mice with kidney-specific inactivation of *Hnf1β* have been previously described (13). All experiments involving animals were conducted under the auspices of the UT Southwestern Institutional Animal Care and Use Committee.

Chromatin Immunoprecipitation—ChIP assays were performed using ChIP-IT® High Sensitivity kits (Active Motif™) or EZ ChIP™ kits (EMD Millipore) according to the manufacturer's protocol. mIMCD3 cells were cross-linked with 1% formaldehyde for 15 min at room temperature. Immunoprecipitation was performed with 5 μg of rabbit anti-HNF-1β antibody, sc-22840 (Santa Cruz), or rabbit IgG, sc-2027 (Santa Cruz), as a negative control. Purified genomic DNA was amplified using specific primers and visualized on 1% agarose gels. The products were normalized relative to 10% of the input DNA.

ChIP Sequencing—Two control (anti-IgG) and two experimental (anti-HNF-1β) samples from the immunoprecipitated DNA from mIMCD3 cells were sent for sequencing using a Solexa platform. Quality assessment of the raw sequencing data was done using FASTQC. Reads with >70% bases with quality lower than Phred score of 20 were removed. Quality score filtered reads were then aligned to the mouse reference genome NCBI37 (mm9) using Burrows-Wheeler aligner. Identification of transcription binding sites was performed using the peak calling algorithm, QuEST. A -fold-change cutoff of three was applied to identify peaks in the experimental ChIP that were significantly above background. The identified peaks were annotated using HOMER. Peaks were mapped to miRNAs if they were located upstream or upstream of an miRNA locus (independent of distance) and no intervening gene was present between the miRNA and the binding site.

MicroRNA Microarrays—53A cells were incubated for 48 h with mifepristone to induce the expression of dominant-negative mutant HNF-1β or vehicle as a control. Total RNA was isolated with miRNeasy Mini kits, and miRNA microarray analysis was performed by LC Sciences (Houston, TX) as previously described (28).

Plasmids—Mouse genomic DNA was amplified using primers 5′-TAGAATACGCGTACAAAGCGGTTCTTGACAGG-3′ and 5′-TAGAATCTCGAGGCTCAGCAGAAAGGGAGAGA-3′, where the underlined sequences are MluI and XhoI sites, respectively. The 2.5-kb PCR product was cloned into pGL3-Basic (Promega) that was previously digested with MluI and XhoI to generate the pGL3-S1S2 plasmid. The HNF-1β sites were mutated to produce the pGL3-mutS1S2 plasmid. The sequences of the primers used to introduce the S1 mutation were 5′-CTGTTTTTTCTCAGAGCAGAA*GTCGGCAGCCGG*TCAACACAAAATTCCTGGGCT-3′ and 5′-AGCCCAGGAATTTTGTGTTGAC*CGGCTGCCGA*CTTCTGCTCTGAGAAAAAACAG-3′. The sequences of the primers used to introduce the S2 mutation were 5′-CTCTTGTGCTTTTCCAAAGG*GTCGGCAGCCGCC*TTTCTCTTCTTGCTTGC-3′ and 5′-GCAAGCAAGAAGAGA-

AAGGCGGCTGCCGACCCTTTGGAAAAGCACAAGAG-3′. The underlined sequences represent the HNF-1β binding site, and the italicized sequences denote the mutated bases. Site-directed mutagenesis was performed as previously described (28). pGL3-FLP S1S2 was constructed by ligating a 2.5-kb mouse genomic PCR product that includes the HNF-1β binding sites into pGL3-Basic that was previously digested with MluI and XhoI. The sequences of the PCR primers were 5′-TAGAATCTCGAGACAAAGCGGTTCTTGACAGG-3′ and 5′-TAGAATACGCGTGCTCAGCAGAAAGGGAGAGA-3′, where the underlined sequences denote the XhoI and MluI sites, respectively.

Luciferase Reporter Assays—53A cells expressing dominant-negative HNF-1β or HeLa cells were plated in 6-well plates (2×10^5 cells/well) and co-transfected with 0.6 μg of the pGL3 plasmids encoding *Photinus* luciferase and 0.02 μg of pRL-CMV encoding *Renilla* luciferase. Cells were harvested 48 h after transfection and lysed in 250 μl of passive lysis buffer. 40 μl of the lysate was added to 96-well plates. *Photinus* and *Renilla* luciferase activities were measured using the Dual Luciferase Reporter Assay system (Promega) according to the manufacturer's directions.

RNA Silencing—On-TARGET plus siRNAs were purchased from Thermo Scientific. Cells (2×10^5cells/well) were seeded in 6-well plates and transfected with a mixture of four siRNAs (80 nM each) using Lipofectamine 2000. The sequences of siRNAs targeting the various regions of the long noncoding RNA are as follows: −25 kb, 5′-PUUAUCUUCCACGUAUUC-UGUU-3′; −14 kb, 5′-PUUUAUAUCAAGGUCUGAGGUU-3′; −10 kb, 5′-PUUGCUCUCUGAGUUCUACCUU-3′; −6.4 kb, 5′-PAUACUGACUGCAUUUGUACUU-3′. An equal amount of non-targeting siRNA (catalogue D-001320-01-05) was used as a control. The cells were harvested 48 h after transfection and lysed in TRIzol.

Overexpression of miR-200—53A cells expressing dominant-negative mutant HNF-1β were stably transfected with plasmids that overexpress mouse miR-200a (catalog #SC400901) and miR-200b (catalog #SC400902) or a control plasmid (catalog #PCMVMIR) using Lipofectamine 2000. Twenty-four hours after transfection, the medium was supplemented with G418 (0.8 μg/ml), and cells were allowed to grow for 12–14 days. The surviving cells were expanded, and the expression of the mature miR-200a and miR-200b transcripts was measured to confirm overexpression.

Western Blots—Total protein was extracted from HNF-1β knock-out and control kidneys. 20 μg of protein was loaded on a 4–15% SDS-polyacrylamide gel, and the proteins were transferred to a nitrocellulose membrane. The membrane was blocked in 5% powdered milk and probed overnight at 4 °C with a primary rabbit anti-Zeb2 antibody (1:1000). Goat-anti rabbit HRP-conjugated IgG was used as a secondary antibody, and the blot was developed using the SuperSignal West Dura Extended Duration substrate from Pierce. The protein bands were quantified using Quantity One imaging software from Bio-Rad.

RNA Isolation and Quantitative RT-PCR—Total RNA was isolated from cultured cells or mouse kidneys using miRNeasy Mini kits (Qiagen). First-strand cDNA was synthesized from mRNA using SuperScript®III Reverse Transcriptase from Life Technologies. The Universal cDNA Synthesis kit from Exiqon was used for first-strand synthesis from miRNA. Quantitative real-time PCR was performed by loading samples in triplicate on a CFX Connect™ Real-time PCR detection system. 18S and 5S RNA were used to normalize expression of mRNA and miRNA, respectively. Data were analyzed using the Bio-Rad CFX software. For semi-quantitative PCR, products were loaded on a 1% agarose gels and stained with ethidium bromide. The images were visualized and analyzed on a Gel Doc™ XR+ system (Bio-Rad). The sequences of the PCR primers are shown in Table 1.

Statistical Analysis—Data are shown as the mean ± S.E. or mean ± S.D. as indicated in the figure legends. Statistical analysis was performed using Student's *t* tests. Analysis of variance followed by Dunnett's post hoc test was used for multiple comparisons.

Results

HNF-1β Regulates Expression of miRNAs in Renal Epithelial Cells—To identify miRNAs that are directly regulated by HNF-1β, we combined chromatin immunoprecipitation and high-throughput sequencing (ChIP-Seq) with miRNA expression profiling. We reasoned that miRNAs that are located near HNF-1β binding sites and show altered expression in cells expressing mutant HNF-1β are likely to represent direct targets, whereas miRNAs that change expression but are not located near binding sites may represent indirect targets. Chromatin from mouse inner medullary collecting duct cells (mIMCD3) was cross-linked and immunoprecipitated with an antibody against HNF-1β. The cross-links were reversed, and the immunoprecipitated DNA was sequenced by next-generation sequencing. Genomic sequences that were enriched by immunoprecipitation with anti-HNF-1β antibody compared with control IgG were mapped on the mouse genome to identify HNF-1β binding sites. The locations of the binding peaks were compared with the locations of miRNAs in the mouse genome. MicroRNAs were selected for further analysis if no other gene was present between the HNF-1β-bound genomic region and the miRNA, unless the miRNA was intragenic. Based on this criterion, we identified 85 miRNAs that were potential HNF-1β targets. HNF-1β binding near representative miRNA targets was verified by chromatin immunoprecipitation (Fig. 1*B*).

To identify miRNAs whose expression is regulated by HNF-1β, we utilized renal epithelial cells expressing an HNF-1β mutant that lacks the C-terminal transactivation domain. Previous studies showed that this protein functions as a dominant-negative mutant (DN-HNF-1β) (29). Cells were treated with mifepristone to induce expression of the DN-HNF-1β mutant or vehicle as a negative control. miRNA microarray analyses identified 22 miRNAs whose expression increased and 30 miRNAs whose expression decreased in cells expressing DN-HNF-1β (Fig. 1*C*). The changes in expression of representative miRNA targets were verified by quantitative real-time PCR (Q-PCR) (Fig. 1*D*). Combining the results from ChIP-Seq and expression profiling identified 22 miRNAs that are directly regulated by HNF-1β, of which 12 were up-regulated and 10 were down-regulated in HNF-1β mutant kidney cells (Fig. 1*A*).

TABLE 1
PCR primers used in this study
F, forward; R, reverse.

Primer ID	Sequence	Product
A	F, 5′-GCTCCCTGGAGGGACTTATC-3′ R, 5′-GGGAAACACCATTTCACCTG-3′	2442 bp
B	F, 5′-GCTTCTGGGAGTCCTTTGTG-3′ R, 5′-ACCATCCCCATTCCTACTCC-3′	1298 bp
C	F, 5′-CCCCTTTTCTCCTCTCAACC-3′ R, 5′-ATTTTCCCCGTCCAAAGAGT-3′	1537 bp
D	F, 5′-GGGGTCAGGGATATTCTGGT-3′ R, 5′-AATCTATGCTGAGGCCGAGA-3′	1565 bp
E	F, 5′-CCTGTCATCAAGGGTAGCAGT-3′ R, 5′-CACAATGCTCAGCTATTCTTGG-3′	1694 bp
F	F, 5′-CAAAGCCCTCTTAGCTTACTGGTT-3′ R, 5′-CACCAAATATGGTACCCATCAAAG-3′	1829 bp
G	F, 5′-CACCAAATATGGTACCCATCAAAGCCTCATAA-3′ R, 5′-TGTTCAGGAAGGGCCTAATG-3′	1247 bp
H	F, 5′-CTGCCCTAGGTTGAGCTTTG-3′ R, 5′GTGGGACATCAGACCGAGTT-3′	1556 bp
I	F, 5′-GCTCATGTCCCTCTCTGCTC-3′ R, 5′-ACCTCATCTTGGTGCCTCTG-3′	2461 bp
J	F, 5′-ACCCCACCTGACCTTTCTCT-3′ R, 5′-GGGTGTCTTTGGTGTTTGCT-3′	1875 bp
K	F, 5′-AAGCAAACCCAGCTTTTTGA-3′ R, 5′-CCCAACCTGTGGTCAGCTAT-3′	1749 bp
L	F, 5′-CCCAGAACTCCATCCTCAAA-3′ R, 5′-CATGTGCAACATGTGACCTTAGGCCTGA-3′	895 bp
M	F, 5′-GTCCTTCTGACCCCAACTACATAC-3′ R, 5′-TATTTCCTTCACTCGTAGTGGACA-3′	957 bp
N	F, 5′-AGAAATAGTAGGTGTTCCAGGATAGTGCTG-3′ R, 5′-AAGTACCTATAGATGCTCCTCTAGCTTTTG-3′	2017 bp
O	F, 5′-ACCTTGCCTTCTCTAGACCAGTTGGCGAGCA-3′ R, 5′-CACCACCCAGCCTCAGTGAAAGAGTAT-3′	1266 bp
P	F, 5′-TCACTCATCCTGTGCCAAATTGAGACAAAG-3′ R, 5′-CAAACGACCCCAGCAATTAGCCAAACCA-3′	1488 bp
Q	F, 5′-GCACTTGAAGGTTGTACACAGGACAGAG-3′ R, 5′-TTTGCAAAGGATATGGAGAGGCATCCATCACCCCATATA-3′	1490 bp
R	F, 5′-CCTCTGTCTGGTGAACTGTGTATT-3′ R, 5′-AAAATGCAGATTCTGTAGGTCCTC-3′	1894 bp
S	F, 5′-TTCATTTCTTGACCTATGGCTGTA-3′ R, 5′-CCAGGCAGTATTAGAGATCAGACA-3′	1890 bp
Upstream of *TTLL10* to miR-200b	F, 5′-CAAATTAGGGTTCTTAGGGCTGTA-3′ R, 5′-CGTCATCATTACCAGGCAGTATTA-3′	4737 bp
TTLL10 exon1	F, 5′-TTAGATGTGGAGCCATCTTGGGCT-3′ R, 5′-TGTATTTCCGGGAATGGCAGGAGT-3′	126 bp
TTLL10 exon3	F, 5′-ACAGAGATGGAAGTGAGGCAC-3′ R, 5′-GCCCTTGAATGGGACAGACAG-3′	102 bp
ChIP primers for S2	F, 5′-AGAAAGGCCCAGTACAGATGAGTTAGTAAT-3′ R, 5′-CTGATACATGTTCTAACTTGAACTCTTGTGCT-3′	120 bp
-25-kb site	F, 5′-CCCCTTTTCTCCTCTCAACC-3′ R, 5′-ACCATCCCCATTCCTACTCC-3′	226 bp
-14-kb site	F, 5′-ACCCCACCTGACCTTTCTCT-3′ R, 5′-ACCTCATCTTGGTGCCTCTG-3′	141 bp
-10-kb site	F, 5′-CAACTACATACTTGGACTGTTTTTGAAGCTTAGATCACAGA-3′ R, 5′-CATGTGCAACATGTGACCTTAGGCCTGA-3′	138 bp
Zeb2	F, 5′-TGCCCAACCATGAGTCCTC-3′ R, 5′-GCTTGCAGAATCTCGCCACT-3′	121 bp
Pkd1	F, 5′-TCTCGGAGCAGAATCAATGCC-3′ R, 5′-CAGAGTTGAGGGACAGTGAGAT-3′	102 bp
18S	F, 5′-GTAACCCGTTGAACCCCATT-3′ R, 5′-CCATCCAATCGGTAGTAGCG-3′	151 bp

miR-200 Levels Are Reduced in HNF-1β Mutant Cells and HNF-1β Knock-out Kidneys—Among the 22 miRNAs that were directly regulated by HNF-1β, three miRNAs (miR-200b, miR-200a, and miR-429) belonged to the miR-200 cluster on mouse chromosome 4 (Fig. 1*C*, *arrows*). Like HNF-1β, the miR-200 cluster has been implicated in PKD and EMT and was, therefore, selected for further study. Q-PCR analysis confirmed that the levels of miR-200b, miR-200a, and miR-429 were reduced 2-fold in cells expressing the DN-HNF-1β mutant (Fig. 2*B*). To verify whether expression changed *in vivo*, Q-PCR was performed on kidneys from mutant mice in which HNF-1β was deleted from renal tubules by Cre/loxP recombination (13). The levels of miR-200b, miR-200a, and miR-429 were significantly reduced in HNF-1β mutant kidneys (Fig. 2*C*). The residual expression likely reflects incomplete deletion of HNF-1β and the contribution of other transcription factors. In contrast, the levels of miR-200c and miR-141, which are located on a different chromosome, were unchanged in DN-HNF-1β-expressing cells and HNF-1β mutant kidneys (Fig. 2, *B* and *C*). The miR-200 cluster containing miR-200b, miR-200a, and miR-429 is located in intron 1 of a host gene, *Ttll10*. However, the expression of *Ttll10* exon 1 and exon 3 was unchanged in DN-HNF-1β-expressing cells and HNF-1β-deficient kidneys (Fig. 2*D*). These results indicate that expression of mutant HNF-1β specifically inhibits the expression of miR-200b, miR-200a, and miR-429 and does not affect the expression of the *Ttll10* host gene.

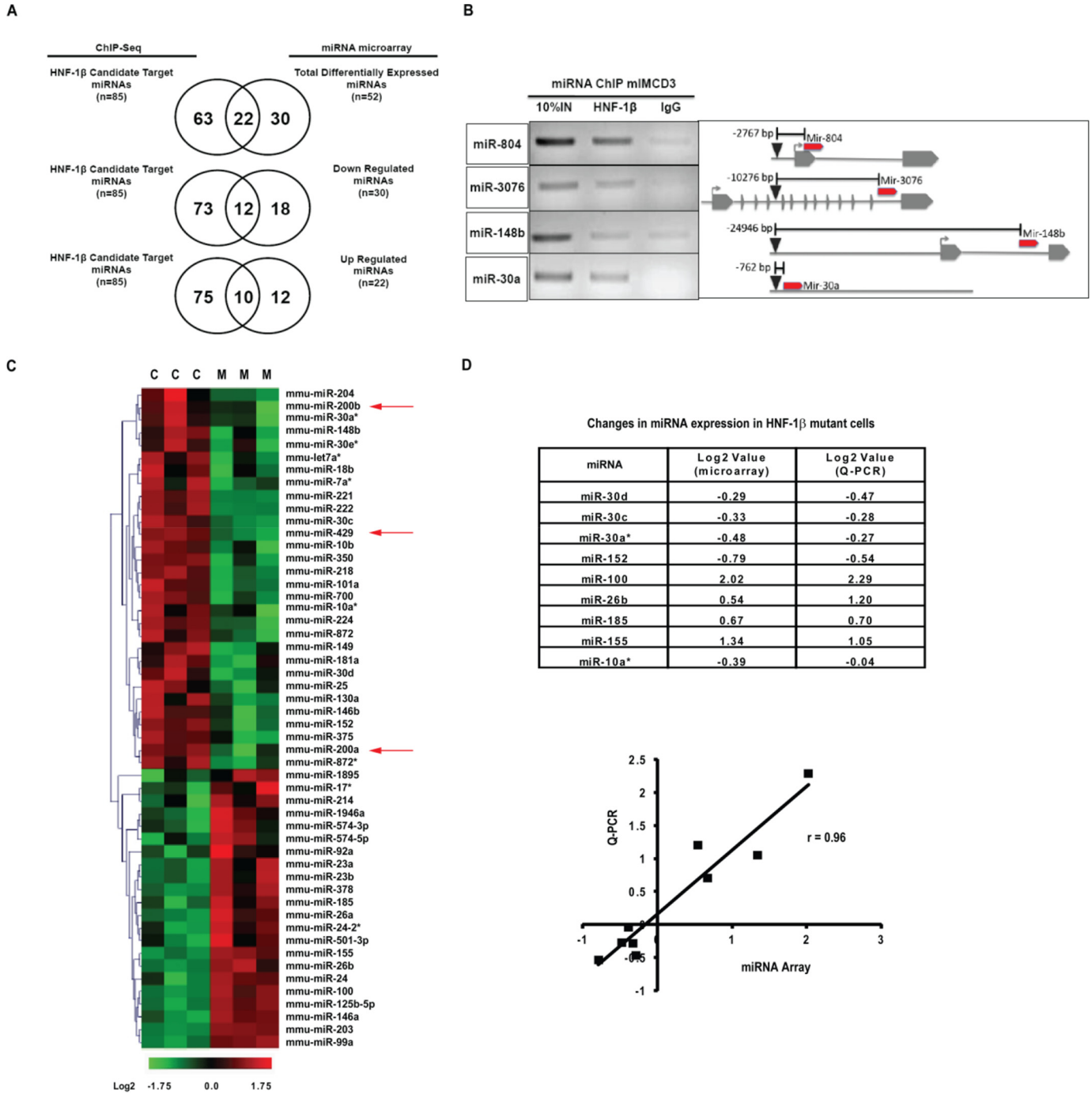

miRNA	Log2 Value (microarray)	Log2 Value (Q-PCR)
miR-30d	-0.29	-0.47
miR-30c	-0.33	-0.28
miR-30a*	-0.48	-0.27
miR-152	-0.79	-0.54
miR-100	2.02	2.29
miR-26b	0.54	1.20
miR-185	0.67	0.70
miR-155	1.34	1.05
miR-10a*	-0.39	-0.04

FIGURE 1. **Identification of miRNAs that are directly regulated by HNF-1β in renal epithelial cells.** *A*, integrated analysis of ChIP-Seq and microarray data to identify miRNAs that are direct targets of HNF-1β. Venn diagrams indicate the number of miRNAs that were mapped near HNF-1β binding sites by ChIP-Seq, the number of miRNAs that showed altered expression in cells expressing the DN-HNF-1β mutant, and the number of miRNAs that were common to both datasets. *B*, chromatin immunoprecipitation showing binding of endogenous HNF-1β near selected miRNA targets in mIMCD3 cells (*left panel*). Immunoprecipitation with IgG was used as a negative control. The *left lanes* contain 10% of the input DNA. The locations of the HNF-1β binding sites (*arrows*) with respect to the miRNAs (*red*) are depicted schematically (*right panel*). *Bracketed lines* indicate distances in base pairs. *C*, heat map showing miRNAs that are differentially regulated in renal epithelial cells expressing dominant-negative mutant HNF-1β (*M*) and uninduced control cells (*C*). Data shown are from three independent experiments. *Arrows* indicate members of the miR-200 cluster. *D*, validation of microarray expression profiling by Q-PCR analysis of representative miRNAs. The change in expression of each miRNA by microarray analysis and Q-PCR is indicated. Scatter plot depicting the correlation between the microarray analysis and Q-PCR is shown in the *lower panel*.

HNF-1β Binds to a Region Located 28 kb Upstream of the miR-200 Locus—ChIP-Seq analysis of chromatin from mIMCD3 renal epithelial cells revealed that HNF-1β binds to a region located 28 kb upstream to miR-200b (Fig. 3*B*). This region contains two evolutionary conserved HNF-1β binding sites, S1 and S2, which are separated by ~1.5 kb (Fig. 3, *B* and *C*). Quantitative ChIP analysis revealed that HNF-1β binding is enriched ~3-fold at the S1 site and 6-fold at the S2 site (Fig. 3*D*). ChIP performed using an antibody that recognizes the phosphorylated C-terminal domain of RNA polymerase II showed enrichment at the S1 and S2 sites, indicating that this region may be transcriptionally active (Fig. 3*E*). Analysis of the mouse

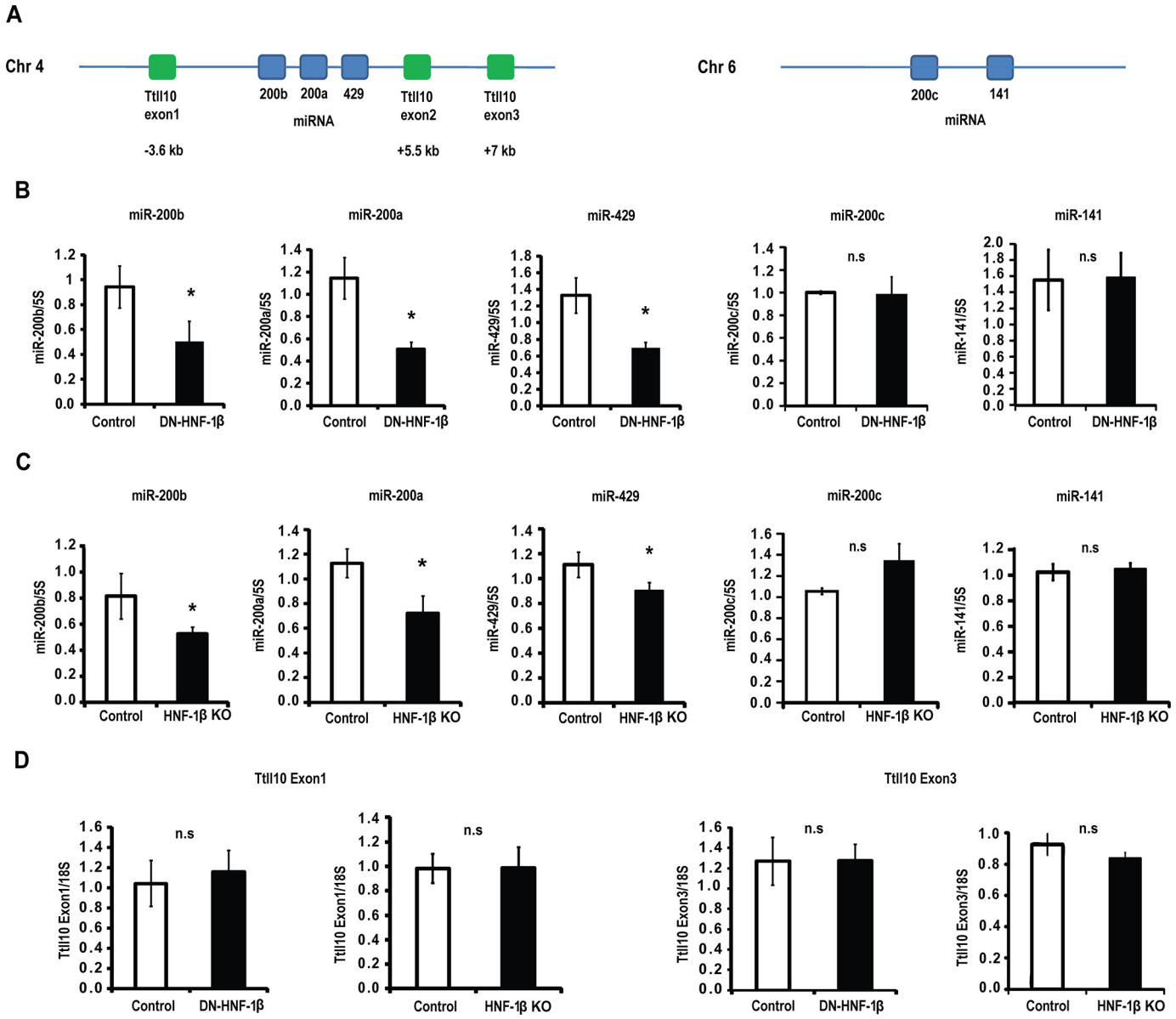

FIGURE 2. **Expression of miR-200 is inhibited by dominant-negative mutant HNF-1β.** *A*, schematic depiction of the mouse miR-200b/200a/429 locus is shown in the *left panel*. The mouse miR-200 cluster (*blue boxes*) is located on chromosome 4 within intron1 of *Ttll10*. The *Ttll10* exons are depicted as *green boxes*, and the distances from miR-200b are indicated *below* (not drawn to scale). Schematic depiction of the mouse miR-200c/141 locus is shown in the *right panel*. The *blue boxes* denote the miRNA cluster (not drawn to scale). *B*, Q-PCR analysis showing levels of mature miR-200b, miR-200a, miR-429, miR-200c, and miR-141 in uninduced cells (*open bars*) and cells expressing the DN-HNF-1β mutant (*solid bars*). *C*, Q-PCR analysis showing levels of miR-200b, miR-200a, miR-429, miR-200c, and miR-141 in kidneys from KspCre;HNF-1$\beta^{fl/fl}$ mice (*solid bars*) and wild-type littermates (*open bars*). The kidneys were analyzed at postnatal day 28. *D*, Q-PCR analysis showing expression of *Ttll10* (exon 1 and exon 3) in cells expressing DN-HNF-1β and kidneys from KspCre;HNF-1$\beta^{fl/fl}$ mice. Data shown represent the mean of three independent experiments. *Error bars* indicate S.E. * indicates $p < 0.05$. *n.s.* indicates non-significant.

ENCODE database indicated that epigenetic marks of active transcription, including H3K4me3, H3K27ac, and H3K4me1, co-localized with the HNF-1β binding sites in adult kidney (Fig. 3*B*). Taken together, these results indicate that the genomic region containing the HNF-1β binding sites is bound by RNA polymerase II and is transcriptionally active.

The −28-kb Site Exhibits HNF-1β-dependent Promoter Activity—To determine if the HNF-1β binding sites at −28 kb are functional, a 2.5-kb genomic fragment containing the S1 and S2 sites was cloned into a promoterless pGL3-Basic luciferase reporter plasmid (Fig. 4*A*). The recombinant plasmid was transfected into HeLa cells, which lack endogenous HNF-1β activity, together with an HNF-1β expression plasmid. HNF-1β transactivated the luciferase reporter plasmid containing the −28 kb sites but had no significant effect on empty pGL3-Basic (Fig. 4*C*). Mutation of the S1 and S2 binding sites (Fig. 4*B*) prevented transactivation by HNF-1β (Fig. 4*C*). When the 2.5-kb genomic DNA fragment was cloned into pGL3-Basic in the reverse orientation, HNF-1β failed to stimulate luciferase activity. These results indicate that the 2.5-kb genomic fragment contains an orientation-dependent promoter. To confirm these findings, the luciferase reporter plasmids were transfected into renal epithelial cells expressing DN-HNF-1β. Transfection of the wild-type plasmid into control (uninduced) cells stimulated luciferase activity, and induction of the DN-HNF-1β mutant inhibited promoter activity (Fig. 4*D*). This

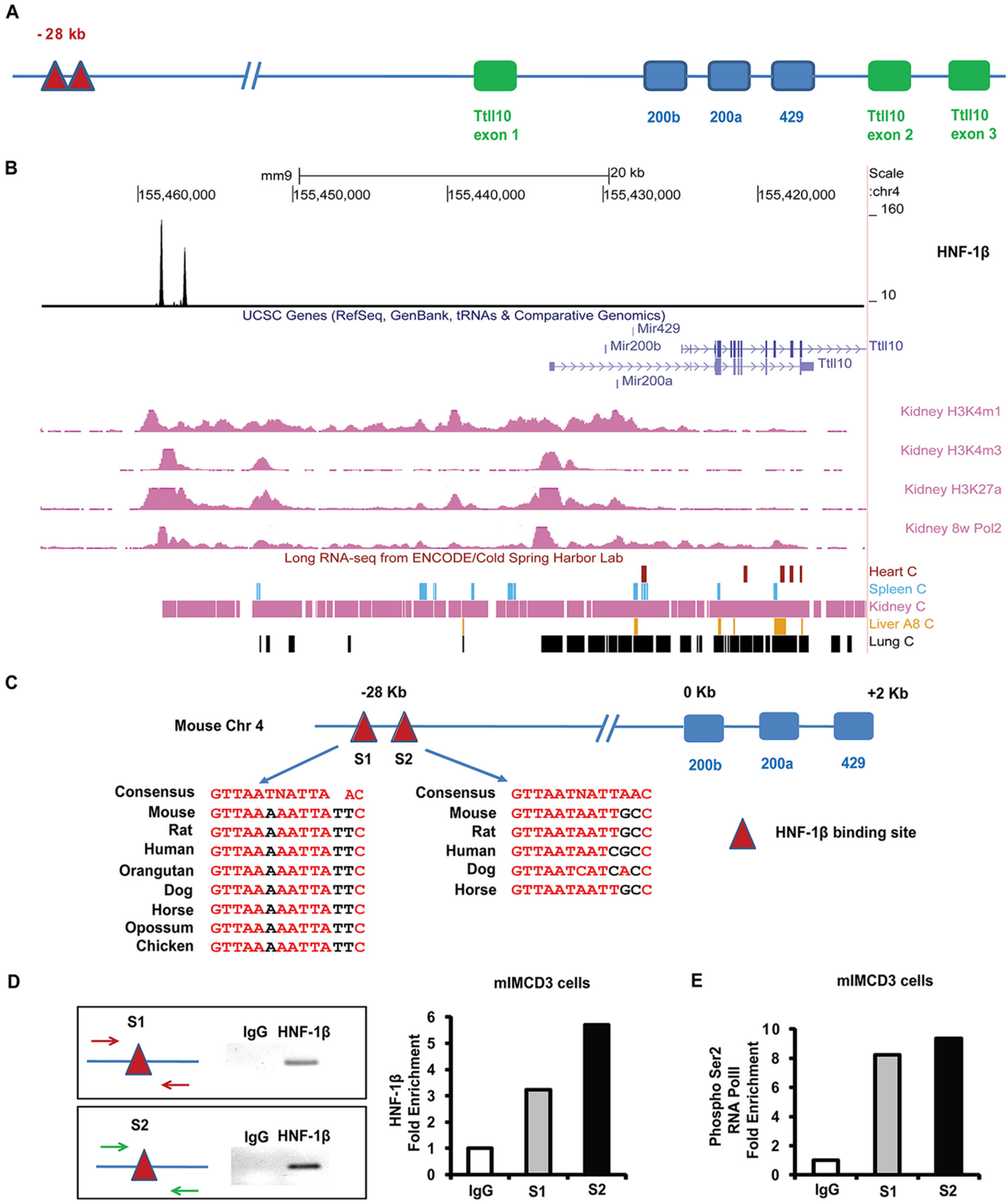

FIGURE 3. **HNF-1β binds 28 kb upstream to miR-200b.** *A*, schematic depiction of the HNF-1β binding sites (*red triangles*) located upstream to the miR-200 locus. *B*, *upper panel*, ChIP-Seq showing the locations of HNF-1β binding sites (*black peaks*) relative to miR-429, miR-200b, miR-200a, and *Ttll10* (*blue lines*) on chromosome 4. Alignments were visualized using the UCSC Genome Browser (53). *Arrows* indicate the direction of transcription. Genomic coordinates and the *size bar* are shown at the *top*. *Middle panel*, *pink peaks* show the locations of histone modifications (*H3K4m1*, *H3K4m3*, *H3K27ac*) and binding of RNA polymerase II (*Pol2*) in chromatin from mouse kidney from the ENCODE database (54). *Lower panel*, alignment with long RNA transcripts in the indicated mouse tissues from ENCODE Cold Spring Harbor Laboratory Long RNA-seq (55). *C*, the S1 and S2 binding sites contain evolutionarily conserved HNF-1β consensus recognition sequences. *D*, validation of the HNF-1β binding at the S1 and S2 sites by chromatin immunoprecipitation. The *arrows* denote the PCR primers. The histograms indicate the -fold enrichment of HNF-1β binding to the S1 and S2 sites compared with IgG control as determined by Q-PCR. *E*, -fold enrichment of the binding of the active form of RNA polymerase II at the S1 and S2 sites compared with control IgG determined by Q-PCR.

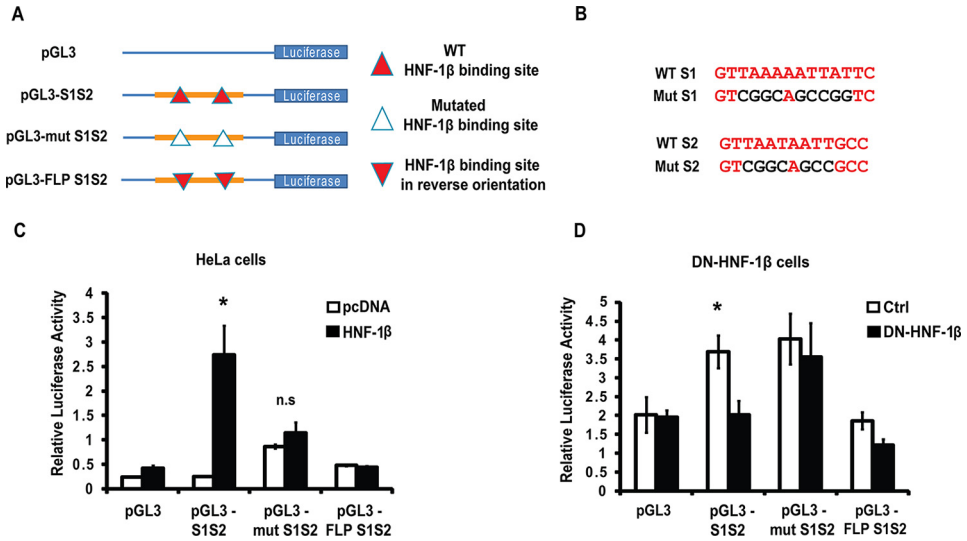

FIGURE 4. **The HNF-1β binding sites are located within a functional promoter.** *A*, schematic diagram of the luciferase reporter plasmids. A 2.5-kb genomic region (*orange bar*) containing the HNF-1β sites was cloned into pGL3-Basic to generate the pGL3-S1S2 plasmid. The *red triangles* denote the conserved HNF-1β binding sites (*S1* and *S2*) located 28 kb upstream to miR-200b. The HNF-1β sites were mutated (*white triangles*) to create the pGL3-mutS1S2 plasmid, and the orientation of the region was reversed in the pGL3-FLP S1S2 plasmid (*inverted red triangles*). *B*, the sequences of the wild-type and mutated S1 and S2 sites are shown. *C*, luciferase activity produced by cotransfection of HeLa cells with the indicated reporter plasmids and an expression plasmid encoding wild-type HNF-1β (*solid bars*) or empty pcDNA (*open bars*). Cells were lysed 48 h after transfection, and *Photinus* luciferase activity was measured relative to *Renilla* luciferase activity. *D*, luciferase activity in uninduced cells (*open bars*) or cells expressing the DN-HNF-1β mutant (*solid bars*) after transfection with the indicated reporter plasmids. Data shown represent the mean of three independent experiments. *Error bars* indicate S.D. * indicates $p < 0.05$. *n.s.* indicates non-significant.

inhibition was blocked by mutation of the HNF-1β binding sites. Transfection of the reporter plasmid containing the genomic fragment in the reverse orientation did not stimulate luciferase activity compared with empty pGL3-Basic. Taken together, these results indicate that the −28-kb region contains a functional promoter that is activated by HNF-1β binding to the S1 and S2 sites.

miR-200 Cluster Is Encoded by a Long Noncoding Transcript—Because the −28-kb region functions as a gene promoter, we investigated whether the transcript that is made from this region encodes the miR-200 cluster. PCR primers were designed to amplify the region between the HNF-1β binding sites and the miR-200b genomic locus. RT-PCR of kidney cDNA produced overlapping PCR products extending from the HNF-1β binding sites to miR-200b (Fig. 5*A*, *upper panel*). As a negative control, primers designed to amplify a region 2-kb upstream to the HNF-1β binding sites did not produce a PCR product. RT-PCR using a forward primer that is upstream to the *Ttll10* promoter and a reverse primer within the miR-200b locus produced a 4.7-kb product in RNA from mIMCD3 cells that was not detected in the absence of reverse transcriptase (Fig. 5*A*, *lower panel*). Collectively, these results identify a long noncoding RNA (lncRNA) transcript extending from the −28-kb site to miR-200b. RT-PCR analysis of various mouse tissues indicated that the expression of the lncRNA transcript was specific to the kidney (Fig. 5*B*).

To determine if HNF-1β regulates the expression of the lncRNA, we designed RT-PCR primers along the length of the transcript and measured the levels in HNF-1β-deficient kidneys. The levels of the lncRNA were decreased 2-fold, indicating that HNF-1β regulates the expression of the lncRNA (Fig. 5*C*). To determine if the lncRNA encodes the miR-200 cluster, four siRNAs that targeted the lncRNA at locations 25, 14, 10, and 6.4 kb upstream to the miR-200 locus were transfected in mIMCD3 cells. RT-PCR analyses showed that the levels of the lncRNA were reduced by 30–40% in mIMCD3 cells transfected with the siRNAs (Fig. 5*D*). Inhibition of the expression of the lncRNA resulted in a corresponding 20–40% reduction in the levels of miR-200b, miR-200a, and miR-429 (Fig. 5*E*). In contrast, the levels of miR-200c, which is located on a different chromosome, were unchanged. Similarly, the levels of *Ttll10* exon1 and exon3 were unchanged by knockdown of the lncRNA (Fig. 5*F*). Taken together, these results indicate that the lncRNA encodes the miR-200b/a/429 cluster but does not encode the *Ttll10* host gene.

HNF-1β Regulates the Expression of Zeb2 and Pkd1 via miR-200—Loss of HNF-1β and miR-200 has been linked to EMT and cystic kidney disease. Because inhibition of HNF-1β leads to reduced levels of miR-200 cluster members, we measured the levels of *Zeb2*, a well established miR-200 target, in HNF-1β mutant cells and kidneys. The expression of *Zeb2* mRNA was increased 2.7-fold in cells expressing DN-HNF-1β and 1.6-fold in HNF-1β mutant kidneys (Fig. 6*A*). Zeb2 protein levels were increased ~2-fold in HNF-1β mutant kidneys (Fig. 6*B*). To determine whether the increase in *Zeb2* was mediated by miR-200, we reexpressed miR-200 in cells expressing DN-HNF-1β. Reexpression of miR-200 prevented the increase in *Zeb2* produced by induction of the DN-HNF-1β mutant (Fig. 6*C*).

We have previously shown that *Pkd1*, which is mutated in autosomal dominant polycystic kidney disease, is post-transcriptionally regulated by miR-200 in kidney cells (28). Therefore, we measured the levels of *Pkd1* mRNA in HNF-1β mutant cells and kidneys. The levels of *Pkd1* mRNA were increased in cells expressing DN-HNF1-β and in HNF-1β-deficient kidneys (Fig. 7*A*). Reexpression of miR-200 in cells expressing

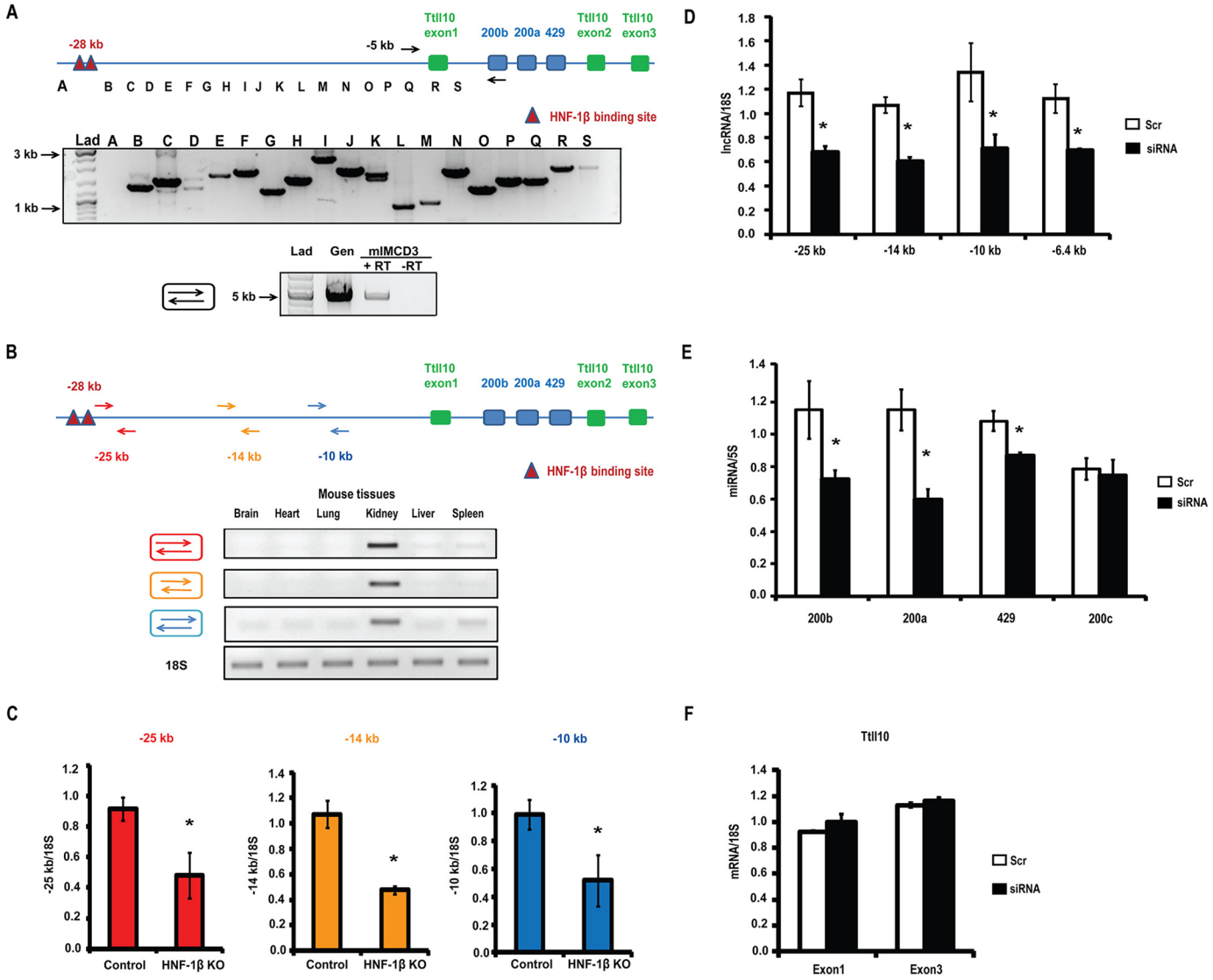

FIGURE 5. **HNF-1β regulates expression of a long noncoding RNA containing the miR-200 cluster.** *A*, *upper panel*, RT-PCR analysis of mouse kidney RNA using overlapping PCR primer sets (*B–S*) designed to amplify the region between the HNF-1β binding sites and miR-200b. The "A" primer set was designed to amplify a region 2-kb upstream to the HNF-1β binding sites. Products were analyzed on a 1% agarose gel and stained with ethidium bromide. PCR products ranging in size from 0.8 to 2.4 kb were obtained from all primer sets except A. *Lower panel*, RT-PCR analysis of mIMCD3 cells using a forward primer upstream of the *Ttll10* promoter and a reverse primer within the miR-200b locus. A 4.7-kb product was detected in RNA from mIMCD3 cells but was not detected in the absence of reverse transcriptase (*RT*). Amplification of genomic DNA (*Gen*) was used as a positive control. *Lad,* size ladder. *B*, RT-PCR analysis of RNA from various mouse tissues using primers (*arrows*) designed to amplify regions located 10, 14, and 25 kb upstream to the miR-200 cluster. The RT-PCR products were analyzed on a 1% agarose gel stained with ethidium bromide. The *lower panel* shows amplification of 18S rRNA. *C*, Q-PCR analysis showing levels of the lncRNA in kidneys from KspCre;HNF-1$\beta^{fl/fl}$ (HNF-1β KO) mice and wild-type littermates (control). *Colored bars* correspond to the regions of the lncRNA shown in *B*. The kidneys were analyzed at postnatal day 28, $n = 3$. *D*, Q-PCR analysis showing levels of the lncRNA in mIMCD3 cells transfected with a mixture of four siRNAs targeting the lncRNA (*solid bars*) or scrambled (*Scr*) siRNA as a control (*open bars*). Primer pairs amplified the indicated regions of the lncRNA. *E*, Q-PCR analysis showing levels of miR-200b, miR-200a, miR-429, and miR-200c in mIMCD3 cells after transfection with siRNA against the lncRNA (*solid bars*) or scrambled siRNA (*open bars*). *F*, expression of mouse *Ttll10* (exon 1 and exon 3) in mIMCD3 cells transfected with siRNA against the lncRNA (*solid bars*) or control scrambled siRNA (*open bars*). Data shown represent the mean of three independent experiments. *Error bars* indicate S.E. * indicates $p < 0.05$.

DN-HNF-1β decreased the levels of *Pkd1* (Fig. 7*B*). These findings indicate that HNF-1β controls the expression of *Zeb2* and *Pkd1* through its regulation of the miR-200 cluster.

Discussion

HNF-1β is a tissue-specific transcription factor that regulates the expression of membrane transporters and other markers of epithelial differentiation in the mammalian nephron. HNF-1β plays a central role in cystic kidney disease genes through its regulation of PKD genes such as *Pkd2* and *Pkhd1*. Here, we identify a novel role of HNF-1β in the regulation of miRNA expression in the kidney. We utilized ChIP-Seq combined with microarray analysis to identify 22 miRNAs that are directly regulated by HNF-1β. Among the direct targets, miR-200b, miR-200a, and miR-429 were of particular interest as they constitute a cluster of miRNAs that is associated with EMT and renal cancer (30–33), both of which have been linked to HNF-1β (22, 34). Like HNF-1β, the expression of miR-200b, miR-200a, and miR-429 is epithelia-specific. In the kidney, miR-200 cluster members are expressed in renal tubules where they are involved in tubular maturation (28). The overlapping patterns of expression suggest that the epithelial tissue-specific

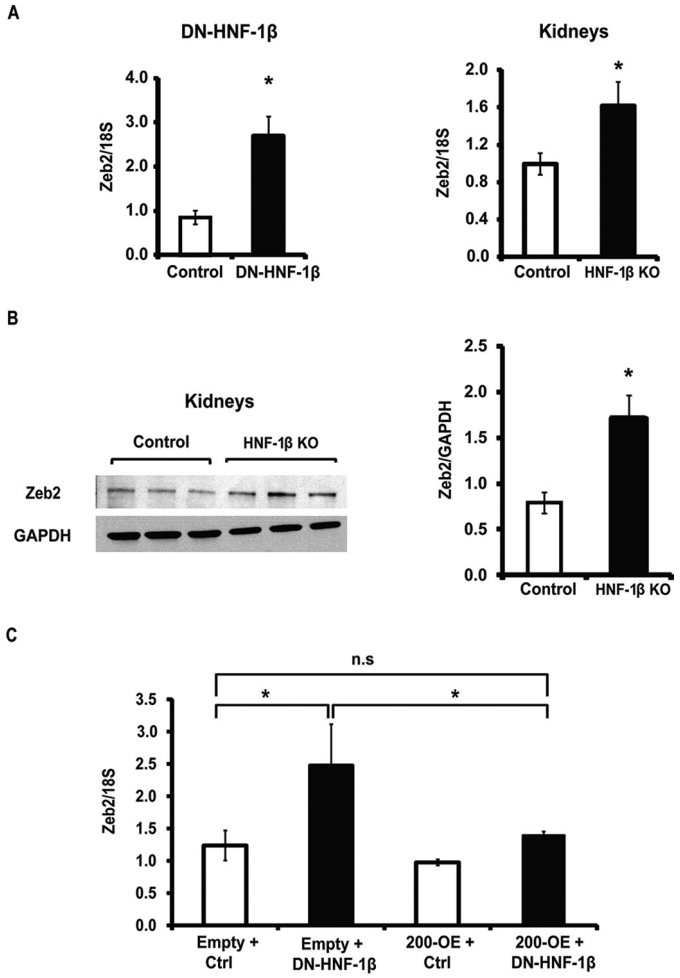

FIGURE 6. **HNF-1β regulates *Zeb2* through miR-200.** *A*, Q-PCR analysis showing levels of *Zeb2* mRNA in cells expressing DN-HNF-1β (*left*) and kidneys from KspCre;HNF-1$\beta^{fl/fl}$ mice (P28, *right*). *B*, Zeb2 protein levels in HNF-1β knock-out kidneys determined by Western blot analysis. The protein bands were quantified using Quantity One imaging software from Bio-Rad. *C*, *Zeb2* mRNA levels in DN-HNF-1β-expressing cells that were stably transfected with empty pCMV (*open bars*) or pCMV-miR-200a/b over-expressing plasmids (*solid bars*). Data shown are the mean of three independent experiments. *Error bars* indicate S.D. *n.s* indicates non-significant. * indicates $p < 0.05$ (analysis of variance).

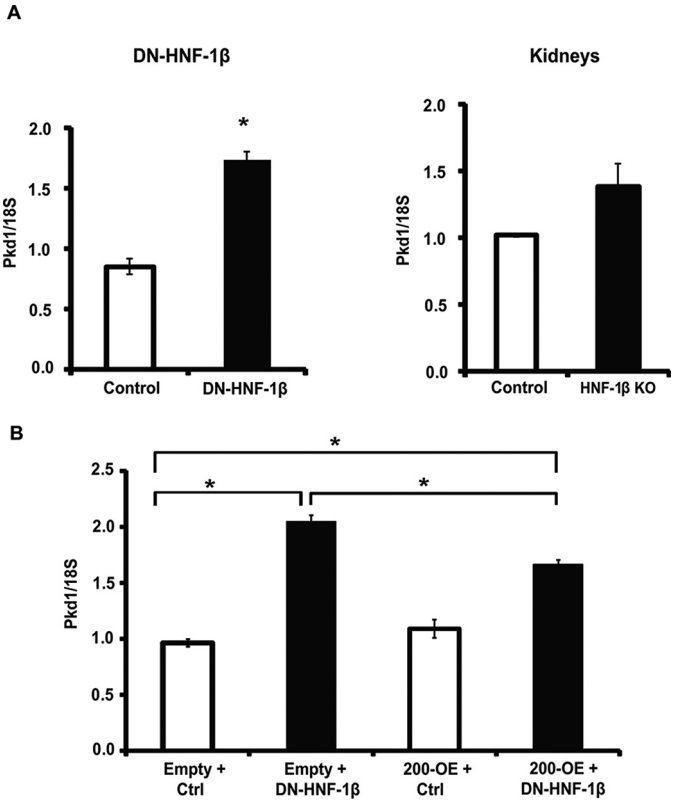

FIGURE 7. **Overexpression of miR-200 decreases *Pkd1* levels in HNF-1β mutant cells.** *A*, *left panel*, Q-PCR analysis of *Pkd1* mRNA levels in cells expressing DN-HNF-1β mutant (*solid bars*) compared with uninduced cells (*open bars*). *Right panel*, *Pkd1* mRNA levels in kidneys from KspCre;HNF-1$\beta^{fl/fl}$ mice (P28, *solid bars*) and wild-type littermates (*open bars*). *B*, *Pkd1* mRNA levels in DN-HNF-1β-expressing cells that were stably transfected with empty pCMV (*open bars*) or pCMV-miR-200a/b overexpressing plasmids (*closed bars*). Data shown are the mean of three independent experiments. *Error bars* indicate S.E. * indicates $p < 0.05$ (analysis of variance).

expression of miR-200 in the kidney is mediated at least in part by HNF-1β. Supporting this conclusion, the expression of miR-200b/a/429 in renal epithelial cells was significantly reduced by inhibition of HNF-1β *in vitro* and *in vivo*. In addition to miR-200, other HNF-1β miRNA targets such as miR-30 are expressed in renal epithelia and are likely to have important functions.

Studies on the mechanism of HNF-1β-dependent regulation of the miR-200 cluster unexpectedly revealed that HNF-1β does not bind near the miR-200 cluster or the promoter of its *Ttll10* host gene. Instead, HNF-1β binds to two evolutionarily conserved sites located 28 kb upstream where it regulates the transcription of a lncRNA that extends to the miR-200b/a/429 cluster. The −28-kb site contains chromatin marks of transcriptional initiation regions of lncRNAs (35) and exhibits HNF-1β-dependent transcriptional activity. Based on our experimental results and data available from the ENCODE consortium, the lncRNA is at least 28 kb in length and is expressed only in the kidney (Figs. 3*B* and 5*B*). This is the first report showing that HNF-1β regulates the expression of a lncRNA. Some tissue-specific lncRNAs have been shown to interact with chromatin-modifying complexes and thereby epigenetically regulate genes involved in cell differentiation (36). Further studies will be needed to determine whether the lncRNA regulated by HNF-1β has similar functions in the kidney.

The long transcript regulated by HNF-1β represents an example of a lncRNA that functions as a pri-miRNA. Supporting this conclusion, the levels of the lncRNA and miR-200b/a/429 cluster are coordinately reduced in HNF-1β mutant cells and kidneys, and siRNA knockdown of the lncRNA leads to a corresponding reduction in the levels of mature miR-200b, miR-200a, and miR-429. Moreover, RT-PCR using a forward primer that is upstream to the *Ttll10* promoter and a reverse primer within the miR-200b locus confirmed the existence of a continuous RNA transcript extending from upstream to the *Ttll10* promoter to the miR-200 cluster. These findings indicate that the lncRNA functions in part as a pri-miRNA that directly encodes the miR-200 cluster. Additional pri-miRNAs encoded by the *Ttll10* host gene may contribute to basal expression of miR-200 but do not appear to be involved in HNF-1β-dependent expression. Recent studies have identified other lncRNAs that are processed to produce miRNAs. For example *H19*

encodes miR-675-3p and miR-675-5p, *linc-MD1* encodes miR-133b, *lnc-31* encodes miR-31, and *Pvt1* encodes miR-1207-50 (37–40). The studies described here add miR-200b/a/429 to the miRNAs that can be produced from a lncRNA.

Besides the miR-200b/a/429 cluster on chromosome 4, the miR-200 family includes the miR-200c/141 cluster located on chromosome 6. In the kidney the transcriptional regulation by HNF-1β appears to be specific to the miR-200b/a/429 cluster as the levels of the miR-200c/141 cluster are unchanged in HNF-1β mutant cells or kidneys. The promoters of the human miR-200b/a/429 and miR-200c/141 clusters have been characterized (41, 42), and transcription factors that regulate expression have been identified, including Sp1, the p53/p63/p73 family, and c-Myb (43–45). These transcription factors may contribute to the residual expression of the miR-200 cluster observed in HNF-1β mutant cells and kidneys (Fig. 2). The human miR-200b/a/429 cluster is located upstream of a protein coding gene, *TTLL10* (tubulin tyrosine ligase-like, member 10), whereas the mouse cluster is located within the first intron of *Ttll10* (Fig. 3*A*). Although the mouse miR-200b/a/429 cluster is intragenic, its HNF-1β-dependent expression appears to be independent of the host gene. In contrast to the miR-200 cluster, the expression of *Ttll10* is unchanged in cells expressing DN-HNF-1β and in HNF-1β-deficient kidneys, and knockdown of the lncRNA does not affect the levels of *Ttll10* transcripts. These findings indicate that HNF-1β regulates the expression of the miR-200 cluster but does not regulate the expression of *Ttll10*.

The miR-200 cluster has been implicated in EMT. Down-regulation of miR-200 in epithelial cells induces EMT, and decreased expression of miR-200 in cancer cells has been linked to increased tumor metastases. Conversely, overexpression of miR-200 members can induce EMT (41, 46). HNF-1β also regulates mesenchymal-to-epithelial transitions. The promoter of the HNF-1β gene (*HNF1B*) contains binding sites for the transcriptional repressor Snail (22). Overexpression of Snail down-regulates HNF-1β, which induces EMT possibly through decreased expression of its target gene, Ksp-cadherin (Cadherin-16). Our studies reveal an alternative mechanism whereby down-regulation of HNF-1β induces EMT. Loss of HNF-1β reduces expression of the lncRNA encoding miR-200 and leads to increased expression of miR-200 targets, including *Zeb2*. Zeb2 is a transcriptional repressor that is sufficient to induce EMT (47). Epithelial cells normally express low levels of *Zeb2*; however HNF-1β-deficient kidneys and cells expressing DN-HNF-1β exhibit increased levels of *Zeb2*. Importantly, overexpression of miR-200a/b in cells expressing DN-HNF-1β restores normal expression of Zeb2, indicating that the increased expression is dependent on miR-200a/b.

We have also uncovered a novel mechanism that links mutations in HNF-1β to cyst formation in the kidney. Previous studies have shown that the expression of *Pkd1*, which is mutated in autosomal dominant polycystic kidney disease, is tightly regulated. Alterations in the levels of *Pkd1*, either transgenic overexpression or expression of hypomorphic alleles, produce kidney cysts (48–52). We found that the expression of *Pkd1* is increased in HNF-1β mutant cells and in kidneys from HNF-1β knock-out mice. However, *Pkd1* does not appear to be a direct transcriptional target of HNF-1β. Rather, HNF-1β regulates the expression of miR-200, which we previously demonstrated controls the post-transcriptional expression of *Pkd1* (28). In support of this mechanism, reexpression of miR-200a/b in HNF-1β mutant cells reduces expression of *Pkd1*. Taken together, our studies identify a novel mechanism by which HNF-1β regulates the expression of *Pkd1* via an lncRNA encoding the miR-200 cluster. Therapeutic approaches that increase the levels of the lncRNA may correct some of the phenotypic abnormalities caused by mutations of HNF-1β.

Author Contributions—S. H., V. P., and P. I. designed the research. S. S. H. performed all research except where otherwise indicated. K. A. performed the ChIP experiments, M. A. analyzed the ChIP-Seq data, and P. C.-S. performed the experiments involving animals. M. P. provided the HNF-1$\beta^{fl/fl}$ mice. S. S. H., V. P., and P. I. analyzed the results. S. S. H. and P. I. wrote the manuscript.

Acknowledgments—We thank Chao Xing and Mohammed Kanchwala in the McDermott Bioinformatics Core at UT Southwestern (National Institutes of Health Grant UL1TR001105) for assistance with data analysis.

References

1. Ott, M. O., Rey-Campos, J., Cereghini, S., and Yaniv, M. (1991) vHNF1 is expressed in epithelial cells of distinct embryonic origin during development and precedes HNF1 expression. *Mech. Dev.* **36,** 47–58
2. Coffinier, C., Barra, J., Babinet, C., and Yaniv, M. (1999) Expression of the vHNF1/HNF1b homeoprotein gene during mouse organogenesis. *Mech. Dev.* **89,** 211–213
3. Mendel, D. B., Hansen, L. P., Graves, M. K., Conley, P. B., and Crabtree, G. R. (1991) HNF-1a and HNF-1b (vHNF-1) share dimerization and homeo domains, but not activation domains, and form heterodimers *in vitro*. *Genes Dev.* **5,** 1042–1056
4. De Simone, V., De Magistris, L., Lazzaro, D., Gerstner, J., Monaci, P., Nicosia, A., and Cortese, R. (1991) LFB3, a heterodimer-forming homeoprotein of the LFB1 family, is expressed in specialized epithelia. *EMBO J.* **10,** 1435–1443
5. Bai, Y., Pontoglio, M., Hiesberger, T., Sinclair, A. M., and Igarashi, P. (2002) Regulation of kidney-specific Ksp-cadherin gene promoter by hepatocyte nuclear factor-1β. *Am. J. Physiol. Renal Physiol* **283,** F839–F851
6. Pontoglio, M., Barra, J., Hadchouel, M., Doyen, A., Kress, C., Bach, J. P., Babinet, C., and Yaniv, M. (1996) Hepatocyte nuclear factor 1 inactivation results in hepatic dysfunction, phenylketonuria, and renal Fanconi syndrome. *Cell* **84,** 575–585
7. Sun, Z., and Hopkins, N. (2001) vhnf1, the MODY5 and familial GCKD-associated gene, regulates regional specification of the zebrafish gut, pronephros, and hindbrain. *Genes Dev.* **15,** 3217–3229
8. Wild, W., Pogge von Strandmann, E., Nastos, A., Senkel, S., Lingott-Frieg, A., Bulman, M., Bingham, C., Ellard, S., Hattersley, A. T., and Ryffel, G. U. (2000) The mutated human gene encoding hepatocyte nuclear factor 1β inhibits kidney formation in developing Xenopus embryos. *Proc. Natl. Acad. Sci. U.S.A.* **97,** 4695–4700
9. Lokmane, L., Heliot, C., Garcia-Villalba, P., Fabre, M., and Cereghini, S. (2010) vHNF1 functions in distinct regulatory circuits to control ureteric bud branching and early nephrogenesis. *Development* **137,** 347–357
10. Massa, F., Garbay, S., Bouvier, R., Sugitani, Y., Noda, T., Gubler, M. C., Heidet, L., Pontoglio, M., and Fischer, E. (2013) Hepatocyte nuclear factor 1β controls nephron tubular development. *Development* **140,** 886–896
11. Igarashi, P., Whyte, D. A., Li, K., and Nagami, G. T. (1996) Cloning and kidney cell-specific activity of the promoter of the murine renal Na-K-C1 cotransporter gene. *J. Biol. Chem.* **271,** 9666–9674
12. Zhang, Y., Wada, J., Yasuhara, A., Iseda, I., Eguchi, J., Fukui, K., Yang, Q., Yamagata, K., Hiesberger, T., Igarashi, P., Zhang, H., Wang, H., Akagi, S.,

Kanwar, Y. S., and Makino, H. (2007) The role for HNF-1β-targeted collectrin in maintenance of primary cilia and cell polarity in collecting duct cells. *PLoS ONE* **2,** e414
13. Gresh, L., Fischer, E., Reimann, A., Tanguy, M., Garbay, S., Shao, X., Hiesberger, T., Fiette, L., Igarashi, P., Yaniv, M., and Pontoglio, M. (2004) A transcriptional network in polycystic kidney disease. *EMBO J.* **23,** 1657–1668
14. Kikuchi, R., Kusuhara, H., Hattori, N., Shiota, K., Kim, I., Gonzalez, F. J., and Sugiyama, Y. (2006) Regulation of the expression of human organic anion transporter 3 by hepatocyte nuclear factor 1α/β and DNA methylation. *Mol. Pharmacol.* **70,** 887–896
15. Kikuchi, R., Kusuhara, H., Hattori, N., Kim, I., Shiota, K., Gonzalez, F. J., and Sugiyama, Y. (2007) Regulation of tissue-specific expression of the human and mouse urate transporter 1 gene by hepatocyte nuclear factor 1 α/β and DNA methylation. *Mol. Pharmacol.* **72,** 1619–1625
16. Saji, T., Kikuchi, R., Kusuhara, H., Kim, I., Gonzalez, F. J., and Sugiyama, Y. (2008) Transcriptional regulation of human and mouse organic anion transporter 1 by hepatocyte nuclear factor 1 α/β. *J. Pharmacol. Exp. Ther.* **324,** 784–790
17. Jin, L., Kikuchi, R., Saji, T., Kusuhara, H., and Sugiyama, Y. (2012) Regulation of tissue-specific expression of renal organic anion transporters by hepatocyte nuclear factor 1 α/β and DNA methylation. *J. Pharmacol. Exp. Ther.* **340,** 648–655
18. Cheret, C., Doyen, A., Yaniv, M., and Pontoglio, M. (2002) Hepatocyte nuclear factor 1α controls renal expression of the Npt1-Npt4 anionic transporter locus. *J. Mol. Biol.* **322,** 929–941
19. Bingham, C., and Hattersley, A. T. (2004) Renal cysts and diabetes syndrome resulting from mutations in hepatocyte nuclear factor-1β. *Nephrol. Dial. Transplant.* **19,** 2703–2708
20. Hiesberger, T., Bai, Y., Shao, X., McNally, B. T., Sinclair, A. M., Tian, X., Somlo, S., and Igarashi, P. (2004) Mutation of hepatocyte nuclear factor-1{β} inhibits Pkhd1 gene expression and produces renal cysts in mice. *J. Clin. Invest.* **113,** 814–825
21. Hiesberger, T., Shao, X., Gourley, E., Reimann, A., Pontoglio, M., and Igarashi, P. (2005) Role of the hepatocyte nuclear factor-1β (HNF-1β) C-terminal domain in Pkhd1 (ARPKD) gene transcription and renal cystogenesis. *J. Biol. Chem.* **280,** 10578–10586
22. Boutet, A., De Frutos, C. A., Maxwell, P. H., Mayol, M. J., Romero, J., and Nieto, M. A. (2006) Snail activation disrupts tissue homeostasis and induces fibrosis in the adult kidney. *EMBO J.* **25,** 5603–5613
23. Lee, Y., Jeon, K., Lee, J. T., Kim, S., and Kim, V. N. (2002) MicroRNA maturation: stepwise processing and subcellular localization. *EMBO J.* **21,** 4663–4670
24. Olsen, P. H., and Ambros, V. (1999) The lin-4 regulatory RNA controls developmental timing in *Caenorhabditis elegans* by blocking LIN-14 protein synthesis after the initiation of translation. *Dev. Biol.* **216,** 671–680
25. Galasso, M., Sana, M. E., and Volinia, S. (2010) Non-coding RNAs: a key to future personalized molecular therapy? *Genome Med.* **2,** 12
26. Patel, V., Williams, D., Hajarnis, S., Hunter, R., Pontoglio, M., Somlo, S., and Igarashi, P. (2013) miR-17∼92 miRNA cluster promotes kidney cyst growth in polycystic kidney disease. *Proc. Natl. Acad. Sci. U.S.A.* **110,** 10765–10770
27. Pandey, P., Brors, B., Srivastava, P. K., Bott, A., Boehn, S. N., Groene, H. J., and Gretz, N. (2008) Microarray-based approach identifies microRNAs and their target functional patterns in polycystic kidney disease. *BMC Genomics* **9,** 624
28. Patel, V., Hajarnis, S., Williams, D., Hunter, R., Huynh, D., and Igarashi, P. (2012) MicroRNAs regulate renal tubule maturation through modulation of Pkd1. *J. Am. Soc. Nephrol.* **23,** 1941–1948
29. Ma, Z., Gong, Y., Patel, V., Karner, C. M., Fischer, E., Hiesberger, T., Carroll, T. J., Pontoglio, M., and Igarashi, P. (2007) Mutations of HNF-1β inhibit epithelial morphogenesis through dysregulation of SOCS-3. *Proc. Natl. Acad. Sci. U.S.A.* **104,** 20386–20391
30. Spaderna, S., Brabletz, T., and Opitz, O. G. (2009) The miR-200 family: central player for gain and loss of the epithelial phenotype. *Gastroenterology* **136,** 1835–1837
31. Cano, A., and Nieto, M. A. (2008) Non-coding RNAs take centre stage in epithelial-to-mesenchymal transition. *Trends Cell Biol.* **18,** 357–359
32. Yoshino, H., Enokida, H., Itesako, T., Tatarano, S., Kinoshita, T., Fuse, M., Kojima, S., Nakagawa, M., and Seki, N. (2013) Epithelial-mesenchymal transition-related microRNA-200s regulate molecular targets and pathways in renal cell carcinoma. *J. Hum. Genet.* **58,** 508–516
33. Duns, G., van den Berg, A., van Dijk, M. C., van Duivenbode, I., Giezen, C., Kluiver, J., van Goor, H., Hofstra, R. M., van den Berg, E., and Kok, K. (2013) The entire miR-200 seed family is strongly deregulated in clear cell renal cell cancer compared to the proximal tubular epithelial cells of the kidney. *Genes Chromosomes Cancer* **52,** 165–173
34. Rebouissou, S., Vasiliu, V., Thomas, C., Bellanné-Chantelot, C., Bui, H., Chrétien, Y., Timsit, J., Rosty, C., Laurent-Puig, P., Chauveau, D., and Zucman-Rossi, J. (2005) Germline hepatocyte nuclear factor 1α and 1β mutations in renal cell carcinomas. *Hum. Mol. Genet.* **14,** 603–614
35. Marques, A. C., Hughes, J., Graham, B., Kowalczyk, M. S., Higgs, D. R., and Ponting, C. P. (2013) Chromatin signatures at transcriptional start sites separate two equally populated yet distinct classes of intergenic long noncoding RNAs. *Genome Biol.* **14,** R131
36. Flynn, R. A., and Chang, H. Y. (2014) Long noncoding RNAs in cell-fate programming and reprogramming. *Cell Stem Cell* **14,** 752–761
37. Dey, B. K., Pfeifer, K., and Dutta, A. (2014) The H19 long noncoding RNA gives rise to microRNAs miR-675-3p and miR-675-5p to promote skeletal muscle differentiation and regeneration. *Genes Dev.* **28,** 491–501
38. Legnini, I., Morlando, M., Mangiavacchi, A., Fatica, A., and Bozzoni, I. (2014) A feedforward regulatory loop between HuR and the long noncoding RNA linc-MD1 controls early phases of myogenesis. *Mol. Cell* **53,** 506–514
39. Ballarino, M., Cazzella, V., D'Andrea, D., Grassi, L., Bisceglie, L., Cipriano, A., Santini, T., Pinnarò, C., Morlando, M., Tramontano, A., and Bozzoni, I. (2015) Novel Long Noncoding RNAs (lncRNAs) in Myogenesis: a miR-31 Overlapping lncRNA transcript controls myoblast differentiation. *Mol. Cell. Biol.* **35,** 728–736
40. Alvarez, M. L., Khosroheidari, M., Eddy, E., and Kiefer, J. (2013) Role of microRNA 1207–5P and its host gene, the long non-coding RNA Pvt1, as mediators of extracellular matrix accumulation in the kidney: implications for diabetic nephropathy. *PLoS ONE* **8,** e77468
41. Burk, U., Schubert, J., Wellner, U., Schmalhofer, O., Vincan, E., Spaderna, S., and Brabletz, T. (2008) A reciprocal repression between ZEB1 and members of the miR-200 family promotes EMT and invasion in cancer cells. *EMBO Rep.* **9,** 582–589
42. Bracken, C. P., Gregory, P. A., Kolesnikoff, N., Bert, A. G., Wang, J., Shannon, M. F., and Goodall, G. J. (2008) A double-negative feedback loop between ZEB1-SIP1 and the microRNA-200 family regulates epithelial-mesenchymal transition. *Cancer Res.* **68,** 7846–7854
43. Pieraccioli, M., Imbastari, F., Antonov, A., Melino, G., and Raschellà, G. (2013) Activation of miR200 by c-Myb depends on ZEB1 expression and miR200 promoter methylation. *Cell Cycle* **12,** 2309–2320
44. Kolesnikoff, N., Attema, J. L., Roslan, S., Bert, A. G., Schwarz, Q. P., Gregory, P. A., and Goodall, G. J. (2014) Specificity protein 1 (Sp1) maintains basal epithelial expression of the miR-200 family: implications for epithelial-mesenchymal transition. *J. Biol. Chem.* **289,** 11194–11205
45. Knouf, E. C., Garg, K., Arroyo, J. D., Correa, Y., Sarkar, D., Parkin, R. K., Wurz, K., O'Briant, K. C., Godwin, A. K., Urban, N. D., Ruzzo, W. L., Gentleman, R., Drescher, C. W., Swisher, E. M., and Tewari, M. (2012) An integrative genomic approach identifies p73 and p63 as activators of miR-200 microRNA family transcription. *Nucleic Acids Res.* **40,** 499–510
46. Gregory, P. A., Bert, A. G., Paterson, E. L., Barry, S. C., Tsykin, A., Farshid, G., Vadas, M. A., Khew-Goodall, Y., and Goodall, G. J. (2008) The miR-200 family and miR-205 regulate epithelial to mesenchymal transition by targeting ZEB1 and SIP1. *Nat. Cell Biol.* **10,** 593–601
47. Vandewalle, C., Comijn, J., De Craene, B., Vermassen, P., Bruyneel, E., Andersen, H., Tulchinsky, E., Van Roy, F., and Berx, G. (2005) SIP1/ZEB2 induces EMT by repressing genes of different epithelial cell-cell junctions. *Nucleic Acids Res.* **33,** 6566–6578
48. Pritchard, L., Sloane-Stanley, J. A., Sharpe, J. A., Aspinwall, R., Lu, W., Buckle, V., Strmecki, L., Walker, D., Ward, C. J., Alpers, C. E., Zhou, J., Wood, W. G., and Harris, P. C. (2000) A human *PKD1* transgene generates functional polycystin-1 in mice and is associated with a cystic phenotype. *Hum. Mol. Genet.* **9,** 2617–2627

49. Thivierge, C., Kurbegovic, A., Couillard, M., Guillaume, R., Coté, O., and Trudel, M. (2006) Overexpression of PKD1 causes polycystic kidney disease. *Mol. Cell. Biol.* **26,** 1538–1548
50. Kurbegovic, A., Côté, O., Couillard, M., Ward, C. J., Harris, P. C., and Trudel, M. (2010) Pkd1 transgenic mice: adult model of polycystic kidney disease with extrarenal and renal phenotypes. *Hum. Mol. Genet.* **19,** 1174–1189
51. Rossetti, S., Kubly, V. J., Consugar, M. B., Hopp, K., Roy, S., Horsley, S. W., Chauveau, D., Rees, L., Barratt, T. M., van't Hoff, W. G., Niaudet, P., Niaudet, W. P., Torres, V. E., and Harris, P. C. (2009) Incompletely penetrant PKD1 alleles suggest a role for gene dosage in cyst initiation in polycystic kidney disease. *Kidney Int.* **75,** 848–855
52. Hopp, K., Ward, C. J., Hommerding, C. J., Nasr, S. H., Tuan, H. F., Gainullin, V. G., Rossetti, S., Torres, V. E., and Harris, P. C. (2012) Functional polycystin-1 dosage governs autosomal dominant polycystic kidney disease severity. *J. Clin. Invest.* **122,** 4257–4273
53. Kent, W. J., Sugnet, C. W., Furey, T. S., Roskin, K. M., Pringle, T. H., Zahler, A. M., and Haussler, D. (2002) The human genome browser at UCSC. *Genome Res.* **12,** 996–1006
54. ENCODEProjectConsortium (2012) An integrated encyclopedia of DNA elements in the human genome. *Nature* **489,** 57–74
55. Lin, S., Lin, Y., Nery, J. R., Urich, M. A., Breschi, A., Davis, C. A., Dobin, A., Zaleski, C., Beer, M. A., Chapman, W. C., Gingeras, T. R., Ecker, J. R., and Snyder, M. P. (2014) Comparison of the transcriptional landscapes between human and mouse tissues. *Proc. Natl. Acad. Sci. U.S.A.* **111,** 17224–17229